

Amin Saghafi ¹, Anooshirvan Farshidianfar²

An investigation into vibration control of gear bearing systems

Considering the importance of gear systems as one of the important vibration and noise sources in power transmission systems, an active control for suppressing gear vibration is presented in this paper. A gear bearing model is developed and used to design an active control gear-bearing system. Two possible configurations of control system are designed based on active bearing and active gear–shaft torsional coupling to control and reduce the disturbance affecting system components. The controller for computing the actuation force is designed by using the H-infinity control approach. Simulation results indicate that the desired controller can efficiently be used for vibration control of gear bearing systems.

1. Introduction

Meshing gears are one of the important sources of vibration and noise in power transmission systems [1].

Vibration analysis of gear systems has been intensively studied. However, vibration control of gear systems has attracted less attention. Recently, several control techniques have been proposed to control gear vibrations. Most researches have mainly centered on control and isolation of the gearbox body vibrations to reduce vibration, which is transmitted to the supporting structure of the gearbox. In 1997, Sutton et al. [2] proposed an active control of helicopter gearbox, which used three magnetostrictive actuators attached to a supporting structure to attenuate the vibration transmitted through the supporting structure.

With development of vibrations control technology, active vibration control of internal gear system has been considered. Montague et al. [3] proposed an active

✉ Amin Saghafi, e-mails: a.saghafi@birjandut.ac.ir, a.i.saghafi@gmail.com

¹Department of Mechanical Engineering, Birjand University of Technology, Birjand, Iran

²Department of Mechanical Engineering, Ferdowsi University of Mashhad, Mashhad, Iran



control scheme to reduce vibrations transferred from gear set using the feedforward control method. A set of piezoelectric actuators mounted on the gear pair shafts was employed to reduce gear mesh vibration. Up to 70% reduction in gear acceleration was achieved. Rebbechi et al. [4] proposed an adaptive feedforward control method for active control of the gearbox, in which four magnetostrictive actuators were attached at one of the support bearings. An attenuation of 20–28 dB at the first, 5–10 dB at second, and 0–2 dB at third gear mesh frequencies was reported.

Chen and Brennan [5] proposed an active control system that used three magnetostrictive actuators connected on the gear body in order to generate the secondary forces for reducing the meshing gear vibration, and about 7.5 dB amplitude reduction was obtained at the mesh frequency. Li et al. [6] presented an experimental study of active control of internal shaft for reducing gearbox housing responses. A modified Fx-LMS algorithm with a robust frequency estimate method is applied to control the gear housing vibration. The actuation force applied to the internal shaft was provided by using an actuator mounted on the driven shaft. Up to 14 dB reduction in the gear vibration response was reported. Guan et al. [7] investigated an active internal gearbox structure experimentally to reduce vibration response. Guan et al. [8] compared the performance of four actuation schemes for active control of gearbox vibration due to transmission error excitation.

Li et al. [9] designed a gear vibration active control platform. The active control was performed using the Fx-LMS algorithm. Gao et al. [10] presented vibration control of an internal shaft to reduce gear mesh vibration using a modified Fx-LMS control algorithm. Also, in order to suppress the vibrations of multistage gear transmission systems, Sun et al. [11, 12] proposed an active vibration control using piezoelectric actuators acting on the transmission shaft. PID, fuzzy and Fx-LMS algorithms were used to control the fundamental and harmonic vibrations. Wang et al. [13] constructed an experimental platform for active vibration control of the gear system with piezoelectric actuators. The active control was performed using the adaptive fuzzy proportion integration differentiation control algorithm. About 10 dB reduction in housing vibrations was obtained at harmonic frequencies. However, the application of control techniques to gear systems is relatively new, and few studies have been reported. In this paper, an active control of gear-bearing system is presented for suppressing gear mesh vibration response. Accordingly, two possible configurations of control system are designed based on active bearing and active gear–shaft torsional coupling to control and reduce the disturbance affecting system components. One of the ideas in the field of modern control is the use of the H-infinity control technique, which is selected to design the controller. The H-infinity controller design is generally based on minimization of the H-infinity norm of the closed-loop transfer function [14–16]. It can be presented as an optimization problem. Particle swarm optimization (PSO) algorithm is one of the optimization methods, which today has many applications in different branches of science [17–19]. In this study, the PSO algorithm is used to solve the optimization problem.

The outline of the paper is as follows. The dynamic model of gear-bearing system is presented in Section 2. The active controller design for gear-bearing systems based on the H-infinity control approach is formulated in Section 3. Section 4 presents the simulations and performance evaluations of the proposed active controller. Conclusion is presented in Section 5.

2. Model description of the gear bearing system

The gear-bearing dynamic model investigated in this paper is shown in Fig. 1 [20]. The gear mesh is modeled as a pair of rigid disks connected by a damper and spring along the line of action (LOA). r_g and r_p are the base circle radius of gears, (subscripts (g) and (p) indicate the gear and pinion). I_g and I_p are the mass moments of inertia of the gears. c_m and k_m represent the damping coefficient and gear mesh stiffness. The internal displacement excitation $e(t)$, is also applied to represent static transmission error. T_g and T_p represent the external torques acting on the gear and pinion. Output torque T_g is assumed to be constant to simplify the dynamic problem, i.e., $T_g(t) = T_{mg}$. Static transmission error and external torque T_p are expressed in a Fourier form as [21, 22]:

$$e(t) = e \left(t + \frac{2\pi}{\omega_e} \right) = \sum_{r=1}^{\infty} e_r \cos(r\omega_e t + \varphi_{er}), \quad (1)$$

$$T_p(t) = T_{mp} + \sum_{r=1}^{\infty} T_{fpr} \cos(r\omega_p t + \varphi_{pr}). \quad (2)$$

In this model, the gears are maintained by a pair of deformable shafts and bearings, which can be represented by equivalent springs and dampers elements in the LOA, and off-line of action (OLOA), as shown in Fig. 1. The shaft-bearings stiffnesses in LOA are given by k_{px} and k_{gx} , and also k_{py} and k_{gy} are their stiffnesses in OLOA. c_{px} , c_{gx} , c_{py} and c_{gy} represent the bearing damping coefficients

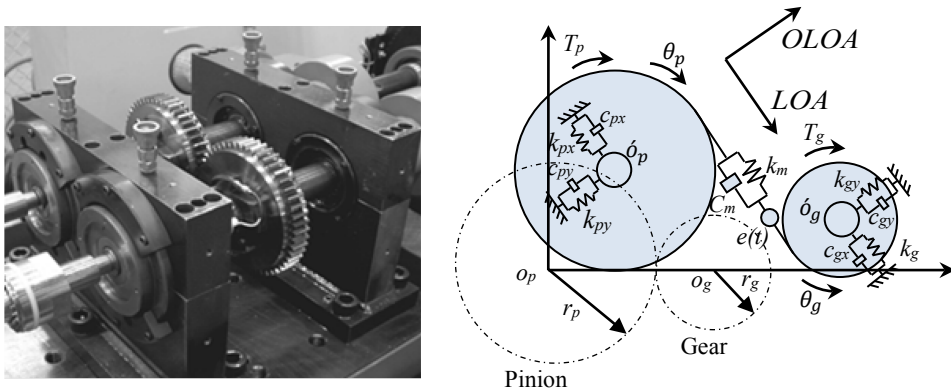


Fig. 1. Schematic of the gear bearing model [20]

of the gears in LOA and OLOA. The centers of the gears are denoted by o_p and o_g , respectively, which are relocated to points \acute{o}_p and \acute{o}_g after the motion. The displacement of the gears is given by translational coordinates x_p , x_g , y_p , and y_g , and rotational coordinate θ_p and θ_g . Under these assumptions, the equations of motion of the gear bearing system can be expressed as:

$$\begin{aligned}
 & I_p \frac{d^2\theta_p}{dt^2} + c_m r_p \left(r_p \frac{d\theta_p}{dt} - r_g \frac{d\theta_g}{dt} + \frac{dx_p}{dt} - \frac{dx_g}{dt} - \frac{de(t)}{dt} \right) \\
 & \quad + k_m r_p (r_p \theta_p - r_g \theta_g + x_p - x_g - e(t)) = T_p, \\
 & I_g \frac{d^2\theta_g}{dt^2} - c_m r_g \left(r_p \frac{d\theta_p}{dt} - r_g \frac{d\theta_g}{dt} + \frac{dx_p}{dt} - \frac{dx_g}{dt} - \frac{de(t)}{dt} \right) \\
 & \quad - k_m r_g (r_p \theta_p - r_g \theta_g + x_p - x_g - e(t)) = -T_g, \\
 & m_p \frac{d^2x_p}{dt^2} + c_m \left(r_p \frac{d\theta_p}{dt} - r_g \frac{d\theta_g}{dt} + \frac{dx_p}{dt} - \frac{dx_g}{dt} - \frac{de(t)}{dt} \right) \\
 & \quad + k_m (r_p \theta_p - r_g \theta_g + x_p - x_g - e(t)) + c_{px} \frac{dx_p}{dt} + k_{px} x_p = 0, \\
 & m_g \frac{d^2x_g}{dt^2} - c_m \left(r_p \frac{d\theta_p}{dt} - r_g \frac{d\theta_g}{dt} + \frac{dx_p}{dt} - \frac{dx_g}{dt} - \frac{de(t)}{dt} \right) \\
 & \quad - k_m (r_p \theta_p - r_g \theta_g + x_p - x_g - e(t)) + c_{gx} \frac{dx_g}{dt} + k_{gx} x_g = 0, \\
 & m_p \frac{d^2y_p}{dt^2} + c_{py} \frac{dy_p}{dt} + k_{py} y_p = 0, \\
 & m_g \frac{d^2y_g}{dt^2} + c_{gy} \frac{dy_g}{dt} + k_{gy} y_g = 0.
 \end{aligned} \tag{3}$$

Eq. (3) can be written into Eq. (4) by introducing a new variable $\delta = r_p \theta_p - r_g \theta_g + x_p - x_g - e(t)$.

$$\begin{aligned}
 & m \frac{d^2\delta}{dt^2} - m \frac{d^2x_p}{dt^2} + m \frac{d^2x_g}{dt^2} + c_m \frac{d\delta}{dt} + k_m(\delta) = \hat{F}_m + \hat{F}_p(t) + \hat{F}_e(t), \\
 & m_p \frac{d^2x_p}{dt^2} + c_m \frac{d\delta}{dt} + k_m(\delta) + c_{px} \frac{dx_p}{dt} + k_{px} x_p = 0, \\
 & m_g \frac{d^2x_g}{dt^2} - c_m \frac{d\delta}{dt} - k_m(\delta) + c_{gx} \frac{dx_g}{dt} + k_{gx} x_g = 0, \\
 & m_p \frac{d^2y_p}{dt^2} + c_{py} \frac{dy_p}{dt} + k_{py} y_p = 0, \\
 & m_g \frac{d^2y_g}{dt^2} + c_{gy} \frac{dy_g}{dt} + k_{gy} y_g = 0,
 \end{aligned} \tag{4}$$

where

$$\hat{F}_m(t) = m \left(\frac{T_{mp} r_p}{I_p} + \frac{T_{mg} r_g}{I_g} \right),$$

$$\hat{F}_e(t) = -m \frac{d^2 e}{dt^2} = \sum_{r=1}^{\infty} (r\omega_e)^2 \hat{F}_{er} \cos(r\omega_e t + \varphi_{er}),$$

$$m = \frac{I_p I_g}{I_g r_p^2 + I_p r_g^2},$$

$$\hat{F}_p(t) = \sum_{r=1}^{\infty} m \left(\frac{r_p}{I_p} \right) T_{fpr} \cos(r\omega_p t + \varphi_{pr}) = \sum_{r=1}^{\infty} \hat{F}_{pr} \cos(r\omega_p t + \varphi_{pr}).$$

Here, m is the equivalent mass, \hat{F}_m is the average force, $\hat{F}_p(t)$ is the fluctuating force from the input excitations, and the internal excitation $\hat{F}_e(t)$ is related to the static transmission error. Equation (4) presents the dynamic equation of a gear-bearing system. This model is employed in order to design an active control system.

3. Active control system schema and control concept

This section presents two applicable models for active control of gear-bearing system. The main purpose of designing this control system is to reduce the vibration response due to disturbances and unwanted design parameters.

In the first proposed concept, an active shaft is presented to reduce the disturbance affecting system components [8]. In this case, actuators are attached between the gear and corresponding shaft for one set of shaft and gear, as shown in Fig. 2. The actuators transfer the torque (T_p), and simultaneously generate excitation torque $u_p(t)$, which represents the component of the active system. A feedback controller

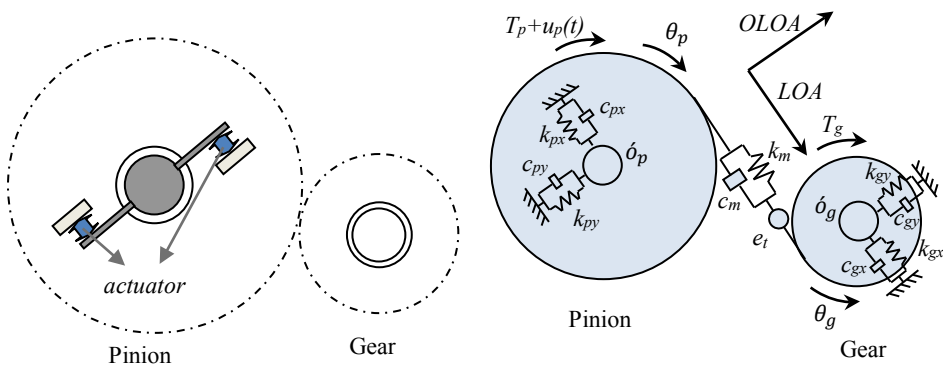


Fig. 2. Schematic of first active gear-bearing model

is employed to determine the appropriate excitation torque of the actuators for suppressing gear mesh vibration response. For this control system, the dynamic equations of the system can be written as:

$$\begin{aligned}
 m \frac{d^2 \delta}{dt^2} - m \frac{d^2 x_p}{dt^2} + m \frac{d^2 x_g}{dt^2} + c_m \frac{d\delta}{dt} + k_m(\delta) &= \hat{F}_m + \hat{F}_p(t) + \hat{F}_e(t) + u(t), \\
 m_p \frac{d^2 x_p}{dt^2} + c_m \frac{d\delta}{dt} + k_m(\delta) + c_{px} \frac{dx_p}{dt} + k_{px} x_p &= 0, \\
 m_g \frac{d^2 x_g}{dt^2} - c_m \frac{d\delta}{dt} - k_m(\delta) + c_{gx} \frac{dx_g}{dt} + k_{gx} x_g &= 0, \\
 m_p \frac{d^2 y_p}{dt^2} + c_{py} \frac{dy_p}{dt} + k_{py} y_p &= 0, \\
 m_g \frac{d^2 y_g}{dt^2} + c_{gy} \frac{dy_g}{dt} + k_{gy} y_g &= 0.
 \end{aligned} \tag{5}$$

Here, the first governing equations for the torsional motion are coupled to the next two equations that represent translations in the LOA direction. The last two equations (translations in the OLOA direction) are uncoupled from the other three coordinates, which can be ignored. In this paper, the static feedback H-infinity control problem is formulated to suppress disturbance. The construction of controller is based on the model shown in Fig. 3. In this control problem, $w(t)$ represents the disturbances, and the control input $u(t) = mu_p(r_p/I_p)$ corresponds to the excitation force. The control objective is to minimize the effect of disturbance on the dynamic responses of the system. Hence, the controller objectives (z), which are used as outputs of the control system, can be stated as transmission error ($\delta(t)$), gear mesh force ($F = k_m \delta(t) + c_m \dot{\delta}(t)$), translation displacements and accelerations of gears (x_p , x_g , \ddot{x}_p , and \ddot{x}_g). Considering practical application, velocity and acceleration of the pinion centers can be easily measured and are proposed as measured outputs (y).

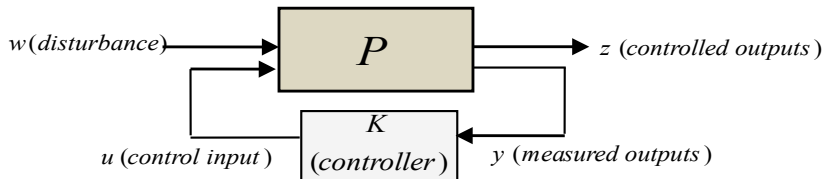


Fig. 3. General structure of control system

Choosing the generalized displacements $x_1 = x_p$, $x_2 = x_g$, $x_3 = \delta(t)$, and velocities $x_4 = \dot{x}_p$, $x_5 = \dot{x}_g$, $x_6 = \dot{\delta}(t)$ as states, and $w(t) = \hat{F}_m + \hat{F}_p + \hat{F}_e$

as disturbances, the gear-bearing control system can be described into the state space as:

$$\begin{aligned}
 \begin{bmatrix} \dot{x}_1 \\ \dot{x}_2 \\ \dot{x}_3 \\ \dot{x}_4 \\ \dot{x}_5 \\ \dot{x}_6 \end{bmatrix} &= \begin{bmatrix} 0 & 0 & 0 & 1 & 0 & 0 \\ 0 & 0 & 0 & 0 & 1 & 0 \\ 0 & 0 & 0 & 0 & 0 & 1 \\ -\frac{k_{px}}{m_p} & 0 & -\frac{k_m}{m_p} & -\frac{c_{px}}{m_p} & 0 & -\frac{c_m}{m_p} \\ 0 & -\frac{k_{gx}}{m_g} & \frac{k_m}{m_g} & 0 & -\frac{c_{gx}}{m_g} & -\frac{c_m}{m_g} \\ -\frac{k_{px}}{m_p} & \frac{k_{gx}}{m_g} & -\frac{k_m}{m} & -\frac{k_m}{m_p} & -\frac{k_m}{m_g} & -\frac{c_{px}}{m_p} & \frac{c_{gx}}{m_g} & -\frac{c_m}{m} & -\frac{c_m}{m_p} & -\frac{c_m}{m_g} \end{bmatrix} \begin{bmatrix} x_1 \\ x_2 \\ x_3 \\ x_4 \\ x_5 \\ x_6 \end{bmatrix} \dots \\
 &\dots + \begin{bmatrix} 0 & 0 & 0 & 0 & 0 & 0 & 0 & 0 & 0 & 0 \end{bmatrix}^T w + \begin{bmatrix} 0 & 0 & 0 & 0 & 0 & 0 & 0 & 0 & 0 & 0 \end{bmatrix}^T u, \quad (6)
 \end{aligned}$$

$$\begin{aligned}
 \begin{bmatrix} z_1 \\ z_2 \\ z_3 \\ z_4 \\ z_5 \\ z_6 \end{bmatrix} &= \begin{bmatrix} 0 & 0 & k_m & 0 & 0 & c_m \\ 1 & 0 & 0 & 0 & 0 & 0 \\ 0 & 0 & 1 & 0 & 0 & 0 \\ 0 & 1 & 0 & 0 & 0 & 0 \\ 0 & -\frac{k_{gx}}{m_g} & \frac{k_m}{m_g} & 0 & -\frac{c_{gx}}{m_g} & \frac{c_m}{m_g} \\ -\frac{k_{px}}{m_p} & 0 & -\frac{k_m}{m_p} & -\frac{c_{px}}{m_p} & 0 & -\frac{c_m}{m_p} \end{bmatrix} \begin{bmatrix} x_1 \\ x_2 \\ x_3 \\ x_4 \\ x_5 \\ x_6 \end{bmatrix} \dots \\
 &\dots + \begin{bmatrix} 0 & 0 & 0 & 0 & 0 & 0 \end{bmatrix}^T w + \begin{bmatrix} 0 & 0 & 0 & 0 & 0 & 0 \end{bmatrix}^T u, \quad (7)
 \end{aligned}$$

$$\begin{aligned}
 \begin{bmatrix} y_1 \\ y_2 \end{bmatrix} &= \begin{bmatrix} -\frac{k_{px}}{m_p} & 0 & -\frac{k_m}{m_p} & -\frac{c_{px}}{m_p} & 0 & -\frac{c_m}{m_p} \\ 0 & 0 & 0 & 1 & 0 & 0 \end{bmatrix} \begin{bmatrix} x_1 \\ x_2 \\ x_3 \\ x_4 \\ x_5 \\ x_6 \end{bmatrix} + \begin{bmatrix} 0 \\ 0 \end{bmatrix} w + \begin{bmatrix} 0 \\ 0 \end{bmatrix} u. \quad (8)
 \end{aligned}$$

We can express (6), (7), and (8) in compact form as:

$$\begin{bmatrix} \dot{x} \\ z \\ y \end{bmatrix} = \begin{bmatrix} A & B_1 & B_2 \\ C_1 & D_{11} & D_{12} \\ C_2 & D_{21} & D_{22} \end{bmatrix} \begin{bmatrix} x \\ w \\ u \end{bmatrix}. \quad (9)$$

In the second proposed model, an active bearing is presented [20]. The main idea is similar to that in an active control model of rotating machinery, as described in Ref. [23]. The central idea of this control is to reduce vibration responses by the excitation forces (or excitation displacements) applied on the bearing. For this purpose, two actuators are placed parallel to LOA between the bearing and the supporting structure, as shown in Fig. 4. The actuator's force ($F_{\text{actuator}} = c_{px}\dot{x}_p + k_{px}x_p + u(t)$), applied on the bearing, is controlled by feedback and represents the component of the active system.

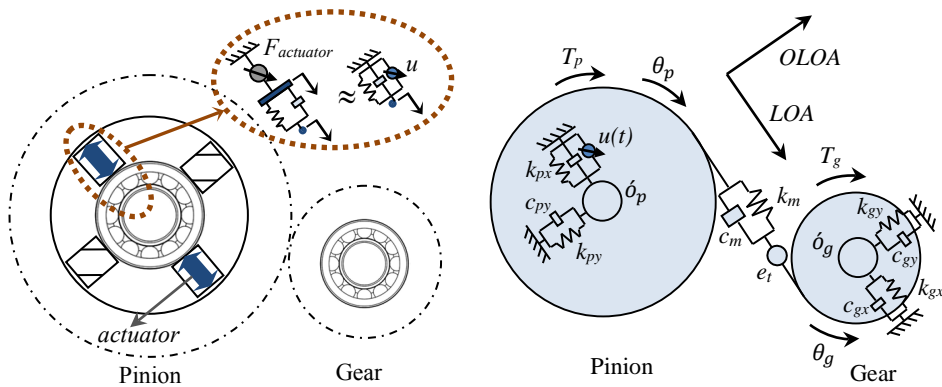


Fig. 4. Schematic of the second active gear-bearing model

For this control system, the controlled output, z , are defined as $\delta(t)$, $F = k_m\delta(t) + c_m\dot{\delta}(t)$, x_p , x_g , \dot{x}_p , and \dot{x}_g . Relative displacement and velocity between the gears centers are proposed as measured output for this active system. Similar to the first concept, by choosing $x_1 = x_p$, $x_2 = x_g$, $x_3 = \delta(t)$, $x_4 = \dot{x}_p$, $x_5 = \dot{x}_g$, $x_6 = \dot{\delta}(t)$ as states, and $w(t) = \hat{F}_m + \hat{F}_p + \hat{F}_e$ as disturbances. Matrices A , B_1 , B_2 , C_1 , C_2 , D_{11} , D_{12} , D_{21} and D_{22} for this model are expressed as:

$$A = \begin{bmatrix} 0 & 0 & 0 & 1 & 0 & 0 \\ 0 & 0 & 0 & 0 & 1 & 0 \\ 0 & 0 & 0 & 0 & 0 & 1 \\ -\frac{k_{px}}{m_p} & 0 & -\frac{k_m}{m_p} & -\frac{c_{px}}{m_p} & 0 & -\frac{c_m}{m_p} \\ 0 & -\frac{k_{gx}}{m_g} & \frac{k_m}{m_g} & 0 & -\frac{c_{gx}}{m_g} & -\frac{c_m}{m_g} \\ -\frac{k_{px}}{m_p} & \frac{k_{gx}}{m_g} & -\frac{k_m}{m} - \frac{k_m}{m_p} - \frac{k_m}{m_g} & -\frac{c_{px}}{m_p} & \frac{c_{gx}}{m_g} & -\frac{c_m}{m} - \frac{c_m}{m_p} - \frac{c_m}{m_g} \end{bmatrix},$$

$$B_1 = \begin{bmatrix} 0 \\ 0 \\ 0 \\ 0 \\ 0 \\ \frac{1}{m} \end{bmatrix}, \quad B_2 = \begin{bmatrix} 0 \\ 0 \\ 0 \\ \frac{1}{m_p} \\ 0 \\ \frac{1}{m_p} \end{bmatrix},$$

$$C_1 = \begin{bmatrix} 0 & 0 & k_m & 0 & 0 & c_m \\ 1 & 0 & 0 & 0 & 0 & 0 \\ 0 & 0 & 1 & 0 & 0 & 0 \\ 0 & 1 & 0 & 0 & 0 & 0 \\ 0 & -\frac{k_{gx}}{m_g} & \frac{k_m}{m_g} & 0 & -\frac{c_{gx}}{m_g} & \frac{c_m}{m_g} \\ -\frac{k_{px}}{m_p} & 0 & -\frac{k_m}{m_p} & -\frac{c_{px}}{m_p} & 0 & -\frac{c_m}{m_p} \end{bmatrix}, \quad D_{11} = \begin{bmatrix} 0 \\ 0 \\ 0 \\ 0 \\ 0 \\ 0 \end{bmatrix},$$

$$D_{12} = \begin{bmatrix} 0 \\ 0 \\ 0 \\ 0 \\ 0 \\ -\frac{1}{m_p} \end{bmatrix}, \quad C_2 = \begin{bmatrix} 1 & -1 & 0 & 0 & 0 & 0 \\ 0 & 0 & 0 & 1 & -1 & 0 \end{bmatrix}, \quad \begin{bmatrix} x_1 \\ x_2 \\ x_3 \\ x_4 \\ x_5 \\ x_6 \end{bmatrix},$$

$$D_{21} = \begin{bmatrix} 0 \\ 0 \end{bmatrix}, \quad D_{22} = \begin{bmatrix} 0 \\ 0 \end{bmatrix}.$$

For the design of a static feedback controller, we consider the following controller K as:

$$u = Ky \implies u = K(I - D_{22}K)^{-1}(C_2x + D_{21}w). \quad (10)$$

Where $K = [k_1 k_2]$ is a feedback control gain to be determined. Substituting (10) into (6) and (7), the closed loop system (9) and so, transfer function of the closed-loop system from w to z are obtained as:

$$\begin{bmatrix} \dot{x} \\ z \end{bmatrix} = \begin{bmatrix} A_{cl} = \mathcal{F}_1 \left[\begin{pmatrix} A & B_2 \\ C_2 & D_{22} \end{pmatrix}, K \right] \\ C_{cl} = \mathcal{F}_1 \left[\begin{pmatrix} C_1 & D_{12} \\ C_2 & D_{22} \end{pmatrix}, K \right] \end{bmatrix} B_{cl} = \mathcal{F}_1 \left[\begin{pmatrix} B_1 & B_2 \\ D_{21} & D_{22} \end{pmatrix}, K \right] D_{cl} = \mathcal{F}_1 \left[\begin{pmatrix} D_{11} & D_{12} \\ D_{21} & D_{22} \end{pmatrix}, K \right] \begin{bmatrix} x \\ w \end{bmatrix}, \quad (11)$$

$$T_{zw}(s) = D_{cl} + C_{cl} (sI - A_{cl})^{-1} B_{cl}, \quad (12)$$

where

$$F_1 \left[\begin{pmatrix} X_{11} & X_{12} \\ X_{21} & X_{22} \end{pmatrix}, Y \right] = X_{11} + X_{12}Y (I - X_{22}Y) X_{21}.$$

The H-infinity controller design is in general based on the minimization of the H-infinity norm of the closed-loop transfer function ($\min. \|T_{zw}(j\omega)\|_\infty$). The objective is to determine the controller gain $K = [k_1 \ k_2]$, such that the closed-loop system would be stable and $\|T_{zw}(j\omega)\|_\infty$ will be the minimum value possible [24]. In view of the limited power of actuators, we cannot consider controller gain more than a given limit. In other words, the controller gain should be limited to a certain range, which is also applied on optimization problem as $\|K\|_\infty \leq K_{\max}$. Thus, the control problem can be briefly summarized as the following constrained optimization problem:

$$\min \left(\|T_{zw}(j\omega | K = [k_1 \ k_2])\|_\infty \right) \quad \text{s. t.} \quad \begin{cases} T_{zw}(s) \text{ is stable,} \\ \|K\|_\infty \leq K_{\max}. \end{cases} \quad (13)$$

To solve the above constrained optimization problem, the PSO method is used. The PSO algorithm can solve complex optimization problems efficiently. In detail, the PSO algorithm employs a swarm of particles which are spread in search space. The performance of each particle is measured based on the objective function. All of the particles share information obtained from the other particles. Communications between the particles cause the search to be efficient. Each particle has two characteristics of velocity (transfer vector), v , and position, x . In initial stage of algorithm, the velocity and position of each particle are initialized by random within the limited ranges. During the evolution process, the position and velocity of each particle are updated. The particles use their memories of the best position experienced so far, x_{best} , and share memories of the best position so far experienced by all particles, $x_{g \text{ best}}$, at every iteration. Then use these memories to regulate their new transfer vectors, and thus further positions. Transfer vector of the i -th particle in $(k+1)$ -th iteration is thus formulated as [16–19]:

$$v_i^j[k+1] = w v_i^j[k] + r_1 c_1 (x_{i, \text{best}}^j[k] - x_i^j[k]) + r_2 c_2 (x_{g \text{ best}}^j[k] - x_i^j[k]), \quad (14)$$

where $i = 1, 2, \dots, n$ (n is the number of particles), $j = 1, 2, \dots, d$ (d stands for the dimension of problem). Coefficient w is called the inertia weight. r_1 and r_2 are also random numbers in the range $[0, 1]$ with uniform distribution. Positive constants c_1 and c_2 are the cognitive and social parameters; usually, the value 2 is suggested for both factors in the literature. The new particle position is updated by adding the updated velocity to the current position according to the following equation (see Fig. 5)

$$x_i^j[k+1] = x_i^j[k] + v_i^j[k+1]. \quad (15)$$

In this way, the particles search for the best solution via the above iterations until convergence to the possible optimum value. In the next section, simulation results are investigated.

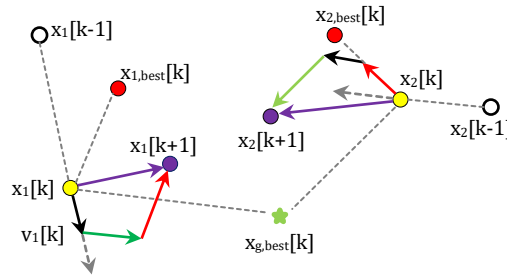


Fig. 5. Movement of particles in PSO algorithm [20]

4. Numerical simulations and performance evaluation

In this section, numerical simulations are presented to demonstrate the performance of the proposed active vibration controller. The simulation parameter values are listed in Table 1. Simulation is done through applying the bounds on the controller gain as, $\|K\|_\infty \leq 10000$ and $\|K\|_\infty \leq 50000$ for model one and $\|K\|_\infty \leq 5000$ and $\|K\|_\infty \leq 100000$ for second model. After solving the optimization problem (13), the controller achieved optimum H-infinity norms of transfer function. The optimum H-infinity norms values and the controller gain values are presented in Table 2.

Table 1.

Parameter values of gear-bearing model

	Mass (kg)	Mass moments inertia (kg m ²)	Base circles diameter (m)	Stiffness coefficient (N/m)	Damping coefficient (N/ms ⁻¹)
Model 1 (Fig. 2)	$m_p = 0.72$ $m_g = 1.98$	$I_p = 8e - 4$ $I_g = 4.8e - 3$	$d_p = 0.07894$ $d_g = 0.12122$	$K_{px} = 5e9$ $K_{gx} = 3e9$ $k_m = 5.68e8$	$C_{px} = 565$ $C_{gx} = 1554$ $c_m = 290$
Model 2 (Fig. 4)	$m_p = 1.18$ $m_g = 1.82$	$I_p = 9.579e - 4$ $I_g = 2.259e - 3$	$d_p = 0.071$ $d_g = 0.0904$	$K_{px} = 3e9$ $K_{gx} = 7e9$ $k_m = 8.88e8$	$C_{px} = 987$ $C_{gx} = 1522$ $c_m = 471$

Performance of the active controller is examined by the frequency analysis. As for the first simulation, the frequency response of the transmission error $\delta(t)$ for model 1, is shown in Fig. 6, where uncontrolled (open-loop) and controlled (closed-loop system for two above controller gains) systems are compared. It is

Table 2.

The optimum H-infinity norms and the controller gain values

	Optimum H-infinity norms of transfer function ($\min \ T_{zw}(j\omega)\ _\infty$)	Controller gain [K]
Model 1	$\ T_{zw}(j\omega)\ _\infty = 15.12$ st. $\ K\ _\infty \leq 10000$	$K_{opt,1} = [1.5651 \ 10000]$
	$\ T_{zw}(j\omega)\ _\infty = 4.95$ st. $\ K\ _\infty \leq 50000$	$K_{opt,2} = [8.8134 \ 50000]$
Model 2	$\ T_{zw}(j\omega)\ _\infty = 20.46$ st. $\ K\ _\infty \leq 5000$	$K_{opt,1} = [-5000 \ 5000]$
	$\ T_{zw}(j\omega)\ _\infty = 6.29$ st. $\ K\ _\infty \leq 100000$	$K_{opt,1} = [98459 \ 29861]$

shown that a considerable reduction of the transmission error is achieved due to disturbances, especially in the range of resonance frequency (around 4890, 7390, and 14200 Hz). Therefore, the performance is improved for the controlled active gear system compared to the uncontrolled system.

On the other hand, the optimization algorithm has found the best solution under higher conditions and converged to the universal optimal control gain, which means an improvement has been achieved. From the results in Fig. 6, it can be seen that the performance of controlled system with control gain $K_{opt,2}$, which has the least value of H-infinity norm, is improved compared with the closed-loop system with control gain $K_{opt,1}$. More precisely, the reduction of maximum transmission error is around 69% for the active system with control gain $K_{opt,1}$, and is also reduced by 89% with higher control condition $K_{opt,2}$.

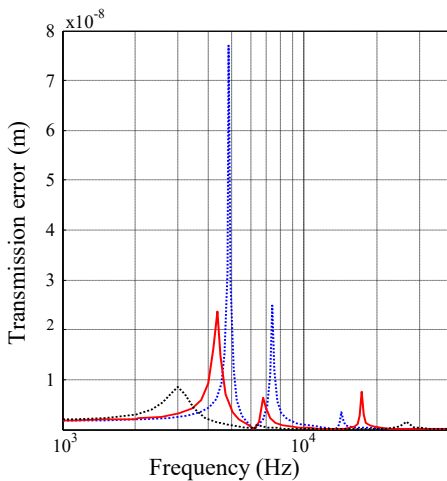


Fig. 6. Frequency response of transmission error to the disturbance input for case 1: uncontrolled system (.....), controlled system with control gain $K_{opt,1}$ (—), and controlled system with control gain $K_{opt,2}$ (- · -)

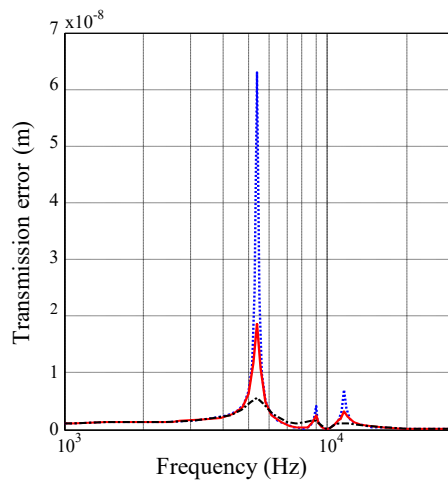


Fig. 7. Frequency response of transmission error to the disturbance input for case 2: uncontrolled system (.....), controlled system with control gain $K_{opt,1}$ (—), and controlled system with control gain $K_{opt,2}$ (- · -)

Furthermore, for model 2, Fig. 7 shows the effect of active control for the transmission error $\delta(t)$. About 70% and 91% of reduction are observed in the maximum response when the active control is applied.

The time-domain responses of the controlled system under random and harmonic excitation are shown in Figs 8–11. It can be seen that an active control system can achieve a lower magnitude for transmission error response when compared with the uncontrolled system. It demonstrates the effectiveness of the active controller for vibration suppression of gear-bearing system. Also, the root-mean-square (RMS) values of the responses are presented in Table 3. These results confirm the observation in Figs 8–11.

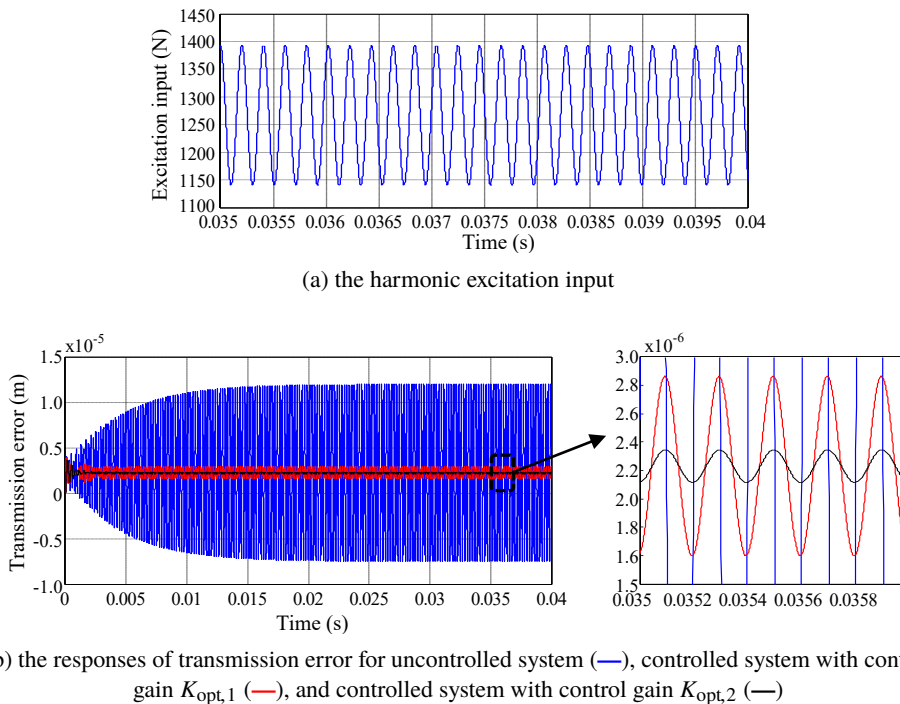


Fig. 8. Transmission error responses under harmonic excitation for model 1

In order to further illustrate, the frequency responses of the displacement and accelerations of gears and also gear mesh force are shown in Figs. 12 and 13. It can be seen from these figures that disturbance rejection can be achieved if the controller is active, especially around the resonances. These diagrams indicate that the H-infinity controller presented in this paper satisfies different objectives, and the disturbances acting on the system are good reduction.

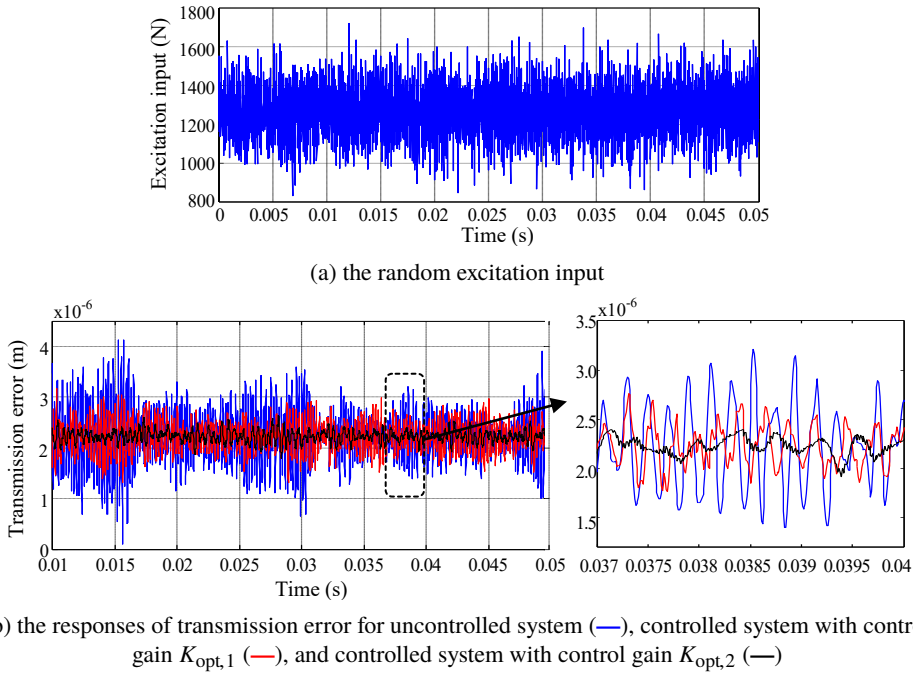


Fig. 9. Transmission error responses under random excitation for model 1

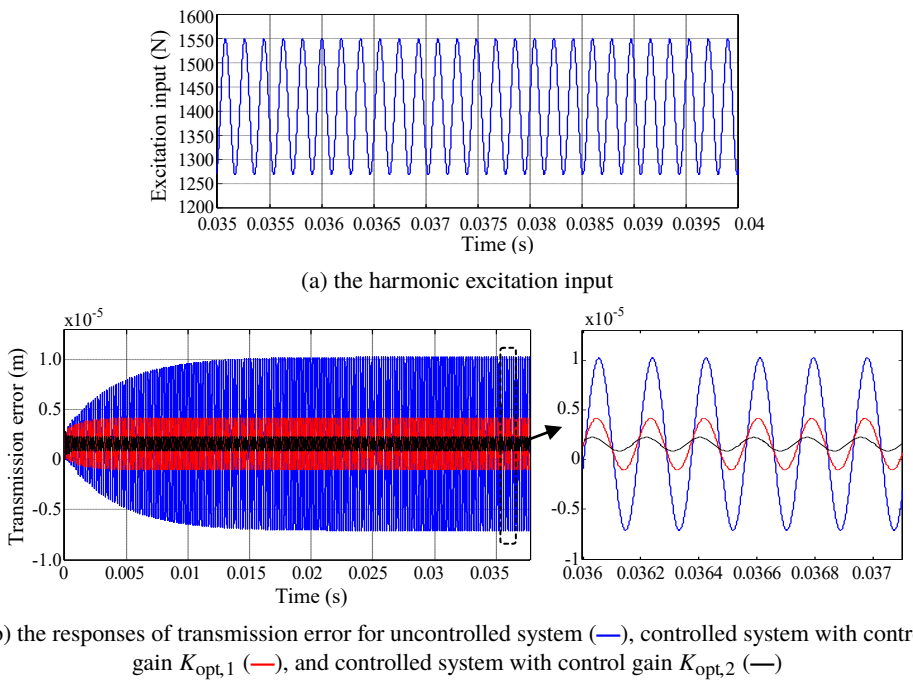


Fig. 10. Transmission error responses under harmonic excitation for model 2

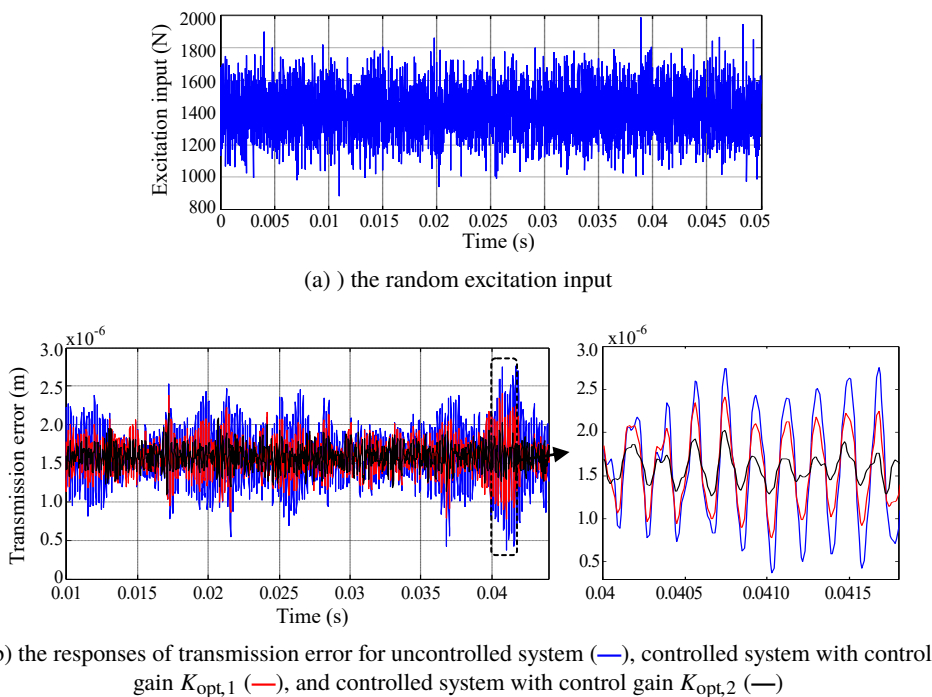


Fig. 11. Transmission error responses under random excitation for model 2

Table 3.

RMS values of the responses

	Model 1			Model 2		
	Uncontrolled system	Controlled system (control gain $K_{opt,1}$)	Controlled system (control gain $K_{opt,2}$)	Uncontrolled system	Controlled system (control gain $K_{opt,1}$)	Controlled system (control gain $K_{opt,2}$)
Transmission error responses under harmonic excitation	0.6702e-5	0.2277e-5	0.2234e-5	0.6296e-5	0.2433e-5	0.1658e-5
Transmission error responses under random excitation	0.2329e-5	0.2248e-5	0.2234e-5	0.1637e-5	0.1604e-5	0.1591e-5

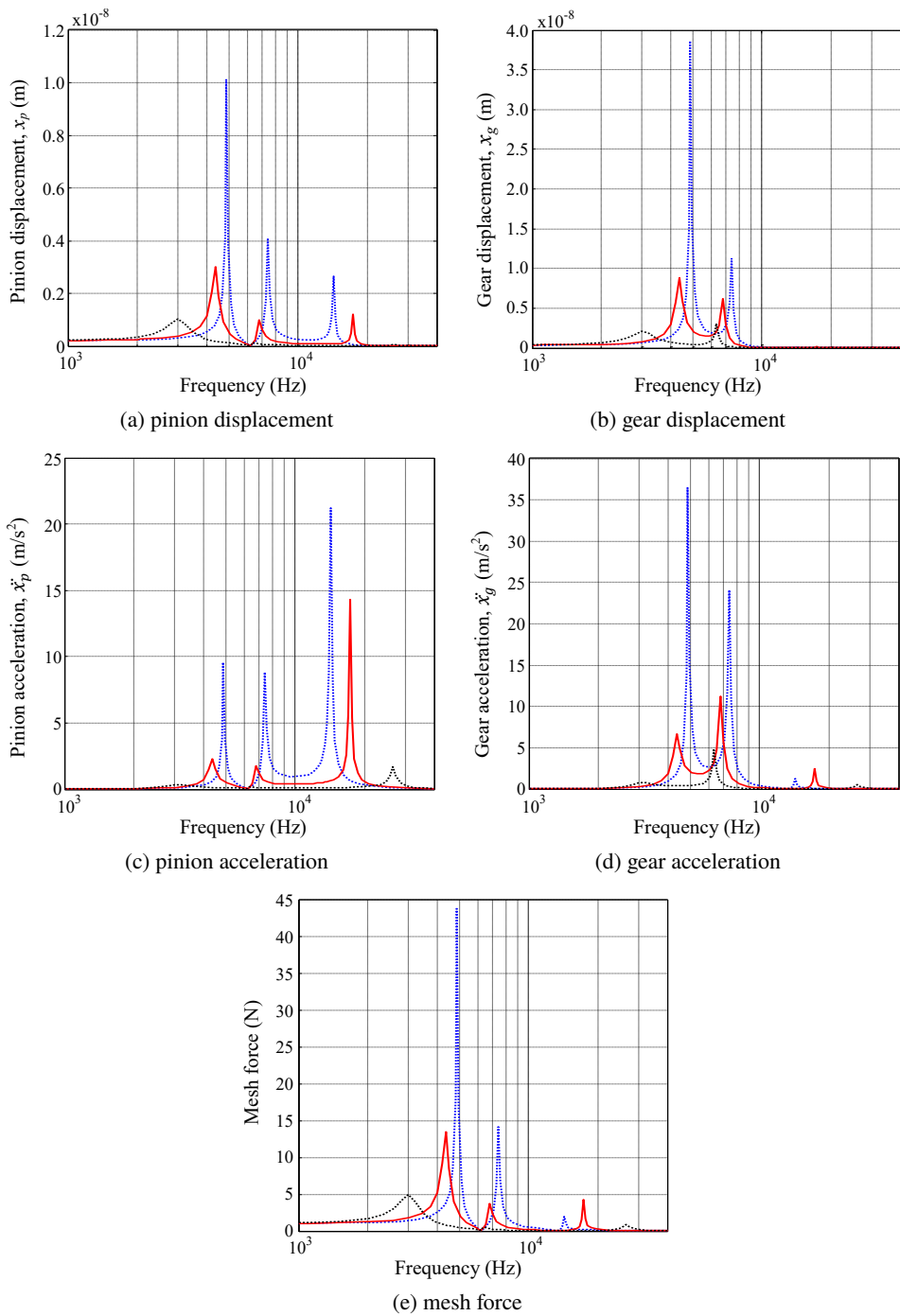


Fig. 12. Frequency response of system to the disturbance input for model 1 for uncontrolled system (.....), controlled system with control gain $K_{opt,1}$ (—), and controlled system with control gain $K_{opt,2}$ (.....)

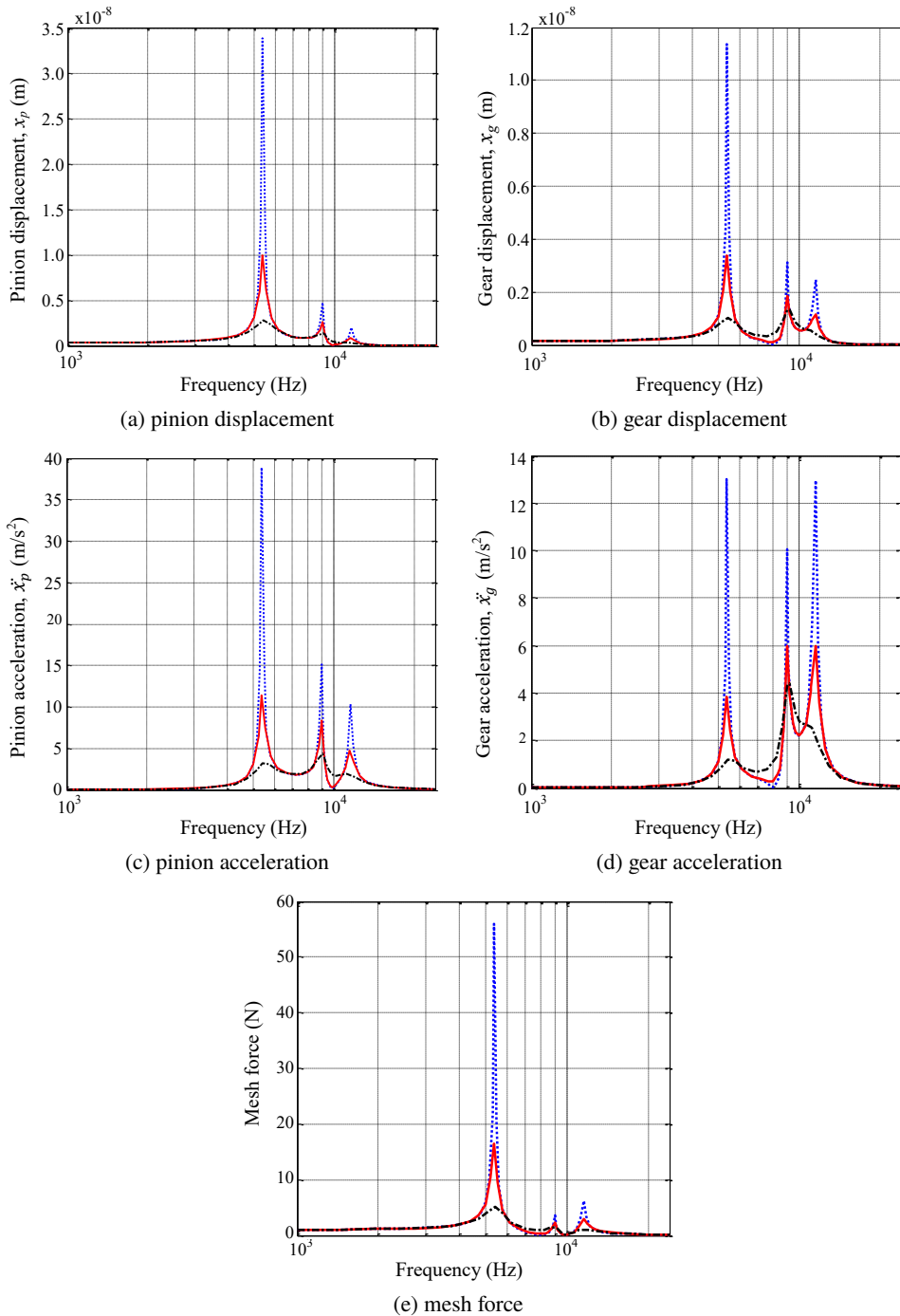


Fig. 13. Frequency response of system to the disturbance input for model 2 for uncontrolled system (.....), controlled system with control gain $K_{opt,1}$ (—), and controlled system with control gain $K_{opt,2}$ (.....)

5. Conclusions

In this paper, an active vibration control system for suppressing gear vibration responses has been presented. Two possible configurations of the control system have been designed based on active bearing and active gear–shaft torsional coupling. An active control based on the H-Infinity feedback controller approach has been presented, and optimizing was performed by using PSO algorithm. The controller’s performance has been validated with numerical simulations. Simulation results show that the controller presented in this paper satisfies the vibration control objectives for disturbance attenuation, which can be utilized to guide experimental studies.

Manuscript received by Editorial Board, March 25, 2021;
final version, September 13, 2021.

References

- [1] H.N. Özgüven and D.R. Houser. Dynamic analysis of high speed gears by using loaded static transmission error. *Journal of Sound and Vibration*, 125(1):383–411, 1988. doi: [10.1016/0022-460X\(88\)90416-6](https://doi.org/10.1016/0022-460X(88)90416-6).
- [2] T.J. Sutton, S.J. Elliott, M.J. Brennan, K.H. Heron and D.A.C. Jessop. Active isolation of multiple structural waves on a helicopter gearbox support strut. *Journal of Sound and Vibration*, 205(1):81–101, 1997. doi: [10.1006/jsvi.1997.0972](https://doi.org/10.1006/jsvi.1997.0972).
- [3] G.T. Montague, A.F. Kaskak, A. Palazzolo, D. Manchala, and E. Thomas. Feed-forward control of gear mesh vibration using piezoelectric actuators. *Shock and Vibration*, 1(5):473–484 1994. doi: [10.3233/SAV-1994-1507](https://doi.org/10.3233/SAV-1994-1507).
- [4] B. Rebbechi, C. Howard, and C. Hansen. Active control of gearbox vibration. *Proceedings of the Active Control of Sound and Vibration Conference*, pages 295–304, Fort Lauderdale, Florida, USA, 02-04 December, 1999.
- [5] M.H. Chen and M.J. Brennan. Active control of gear vibration using specially configured sensors and actuators. *Smart Materials and Structures*, 9:342–350, 2000. doi: [10.1088/0964-1726/9/3/315](https://doi.org/10.1088/0964-1726/9/3/315).
- [6] M. Li, T.C. Lim, and W.S. Shepard Jr. Modeling active vibration control of a geared rotor system. *Smart Materials and Structures*, 13:449–458, 2004. doi: [10.1088/0964-1726/13/3/001](https://doi.org/10.1088/0964-1726/13/3/001).
- [7] Y.H. Guan, T.C. Lim, and W.S. Shepard Jr. Experimental study on active vibration control of a gearbox system. *Journal of Sound and Vibration*, 282(3-5):713–733, 2005. doi: [10.1016/j.jsv.2004.03.043](https://doi.org/10.1016/j.jsv.2004.03.043).
- [8] Y.H. Guan, M. Li, T.C. Lim, and W.S. Shepard Jr. Comparative analysis of actuator concept for active gear pair vibration control. *Journal of Sound and Vibration*, 269(1-2):273–294, 2004. doi: [10.1016/S0022-460X\(03\)00072-5](https://doi.org/10.1016/S0022-460X(03)00072-5).
- [9] Y. Li, F. Zhang, Q. Ding, and L. Wang. Method and experiment study for active vibration control of gear meshing. *Zhendong Gongcheng Xuebao/Journal of Vibration Engineering*, 27(2):215–221, 2014.
- [10] W. Gao, L. Wang, and Y. Liu. A modified adaptive filtering algorithm with online secondary path identification used for suppressing gearbox vibration. *Journal of Mechanical Science and Technology*, 30(11):4833–4843, 2016. doi: [10.1007/s12206-016-1002-z](https://doi.org/10.1007/s12206-016-1002-z).

- [11] W. Sun, F. Zhang, H. Li, H. Wang, and S. Luo. Co-simulation study on vibration control of multistage gear transmission system based on multiple control algorithms. *Proceedings of the 2017 International Conference on Advanced Mechatronic Systems*, pages 1–7, Xiamen, China, 2017. doi:10.1109/ICAMEchS.2017.8316474.
- [12] W. Sun, F. Zhang, W. Zhu, H. Wang, S. Luo, and H. Li. A comparative study based on different control algorithms for suppressing multistage gear transmission system vibrations. *Shock and Vibration*, 2018:ID7984283, 2018. doi: 10.1155/2018/7984283.
- [13] H. Wang, F. Zhang, H. Li, W. Sun, and S. Luo. Experimental analysis of an active vibration frequency control in gearbox. *Shock and Vibration*, 2018:ID7984283, 2018. doi: 10.1155/2018/1402697.
- [14] C. Lauwerys, J. Swevers, and P. Sas. Robust linear control of an active suspension on a quarter car test-rig. *Control Engineering Practice*, 13(5):577–586, 2005. doi: 10.1016/j.conengprac.2004.04.018.
- [15] W. Sun, J. Li, Y. Zhao, and H. Gao. Vibration control for active seat suspension systems via dynamic output feedback with limited frequency characteristic. *Mechatronics*, 21(1):250–260, 2011. doi: 10.1016/j.mechatronics.2010.11.001.
- [16] A. Farshidianfar, A. Saghafi, S.M. Kalami, and I. Saghafi. Active vibration isolation of machinery and sensitive equipment using H_{∞} control criterion and particle swarm optimization method. *Meccanica*, 47:437–453, 2012. doi: 10.1007/s11012-011-9451-z.
- [17] R. Eberhart and J. Kennedy. A new optimizer using particle swarm theory. In *Proceedings of the Sixth International Symposium on Micro Machine and Human Science*, Nagoya, Japan, 4–6 October, 1995. doi: 10.1109/MHS.1995.494215.
- [18] J.F. Schutte and A.A. Groenwold. A study of global optimization using particle swarms. *Journal of Global Optimization*, 31:93–108, 2005. doi: 10.1007/s10898-003-6454-x.
- [19] D. Sedighizadeh and E. Masehian. Particle swarm optimization methods, taxonomy and applications. *International Journal of Computer Theory and Engineering*, 1(5):1793–8201, 2009.
- [20] A. Saghafi, A. Farshidianfar, and A.A. Akbari. Vibrations control of gear-bearing dynamic system. *Modares Mechanical Engineering*, 14(6):135–143, 2014. (in Persian).
- [21] A. Farshidianfar and A. Saghafi. Global bifurcation and chaos analysis in nonlinear vibration of spur gear systems. *Nonlinear Dynamics*, 75:783–806, 2014. doi: 10.1007/s11071-013-1104-4.
- [22] A. Saghafi and A. Farshidianfar. An analytical study of controlling chaotic dynamics in a spur gear system. *Mechanism and Machine Theory*, 96(1):179–191, 2016. doi: 10.1016/j.mechmachtheory.2015.10.002.
- [23] G. Pinte, S. Devos, B. Stallaert, W. Symens, J. Swevers, and P. Sas. A piezo-based bearing for the active structural acoustic control of rotating machinery. *Journal of Sound and Vibration*, 329(9):1235–1253, 2010. doi: 10.1016/j.jsv.2009.10.036.
- [24] S. Skogestad and I. Postlethwaite. *Multivariable Feedback Control: Analysis and Design*. 2nd ed., Wiley Interscience, New York, 2005.